ESRDC Ship Notional Baseline Medium Voltage Direct Current (MVDC) Architecture Thermal Simulation and Visualization

J. V. C. Vargas[1], jvargas@caps.fsu.edu
J. A. Souza[1], souza@caps.fsu.edu
R. Hovsapian[1], hovsapian@caps.fsu.edu
J. C. Ordonez[1], ordonez@caps.fsu.edu
T. Chiocchio[1], chiocchio@caps.fsu.edu
J. Chalfant[2], chalfant@mit.edu
C. Chryssostomidis[2], chrys@mit.edu

[1]Department of Mechanical Engineering and Center for Advanced Power Systems, Florida State University, Tallahassee, Florida, 32310, USA
[2]MIT Sea Grant Design Laboratory, Massachusetts Institute of Technology, Cambridge, Massachusetts 02139, USA

Keywords: MVDC architecture, temperature field, relative humidity field, thermal management, early stage design tool

Abstract

This work presents a fast visualization and thermal simulation tool developed as part of the Electric Ship Research and Development Consortium (ESRDC) funded by the Office of Naval Research (ONR) that is capable of providing quick responses during early stages of ship design. The tool allows for the visualization of thermal and electrical loads, and equipment locations and other variables of interest in the all-electric ship, proceeding to the computation of the resulting whole ship temperature and relative humidity distribution. For that, a previously developed simplified physical model [1-3] – which combines principles of classical thermodynamics and heat transfer, resulting in a system of three-dimensional differential equations which are discretized in space using a three-dimensional cell centered finite volume scheme – is enhanced to include fresh and sea water cooled systems throughout the ship. Therefore, the combination of the proposed simplified physical model with the adopted finite volume scheme for the numerical discretization of the differential equations is called a volume element model (VEM). A 3D simulation is performed in order to determine the temperature distribution inside the ship for the baseline Medium Voltage Direct Current (MVDC) architecture, and representative operating conditions are analyzed. VisIt visualization tool [4] is used to plot the results.

1. INTRODUCTION

The research development of an all electric ship requires the assessment of the integrated systems thermal and electrical response in acceptable conception time. Therefore, a simulation tool that is capable of providing quick responses during early stages of ship design is needed. In this way, thermal viability of the Navy's future all-electric ships could be demonstrated through simulation and modeling at the ship system level. For that, the development of physics-based, electrical-thermal-mechanical models capable of addressing the transient nature of the problem in a global sense is needed.

In that direction, the all electric ship thermal response has been investigated through a simplified physical model in previous studies [1-3]. The model combines principles of classical thermodynamics and heat transfer, resulting in a system of three-dimensional differential equations which are discretized in space using a three-dimensional cell centered finite volume scheme, making use of available empirical and analytical correlations to evaluate required physical quantities such as friction and heat transfer coefficients, and others whenever necessary. Proceeding with the effort, towards the achievement of total ship solutions to thermal and electrical management, a reliable and comprehensive computational visualization tool was also developed [4, 5]. In this way, visualization that geographically lays out a ship's critical thermal management systems and addresses adaptive control issues in a system context will be possible.

It is important to stress that the all-electric ships are expected to make more efficient use of on-board power and to cut fuel use. The technology is also expected to help meet future requirements for high-power weapons such as the electromagnetic gun, high power microwave and high energy lasers. ONR created five "focus areas" for the development of the all-electric ship. They are power gene ration; distribution and control; energy storage; heat transfer and thermal management; and motors and actuators, as reported by Wagner [6]. The five areas are highly interdependent for synchronized and optimal operation. Heat generation is present in all of them, in different levels, from low to high, as a result of electromagnetic launcher operation [7], propulsion [8], and all other ship systems. Therefore poor thermal management could evidently lead to

unexpected and ultimately failure of mechanical-electrical systems to the detriment of the ship's combat mission [9].

A reliable thermal simulation tool makes possible the variation of the system components lay-out such that the total heat generation rate can be increased using the same cooling system. For example, for a given lay-out, based on the resulting temperature field, one could redistribute or even add more components to those regions where the temperatures are lower than the hot-spot temperature, therefore optimizing thermal management for maximum heat dissipation or, in other words, maximizing system power density.

Modern military technology, such as the all electric ship technology by itself poses the maximum power density problem. The task is even more challenging than in civilian applications, since power density increase must be accompanied by a non-revealing equipment thermal signature.

As a result, for the ship's internal and external structure design and optimization, it is desirable that the system mathematical model is as simple as possible. In this way, low computational time to provide solutions for each tested configuration is required, thus allowing for an effective design and optimization procedure.

In this paper, we amend the ship's mathematical model introduced previously [1-3] by extending its capabilities to include fresh and sea water cooled systems throughout the ship, for the assessment of both steady state and transient behaviors. For that, a three dimensional simulation is performed in order to determine the temperature and relative humidity distributions inside the ship for the baseline medium voltage direct current (MVDC) architecture, and representative operating conditions are analyzed.

The present effort is part of the Electric Ship Research and Development Consortium (ESRDC), funded by the Office of Naval Research (ONR).

2. MATHEMATICAL MODEL

Since the main scope of this work is the search for an adequate tool to provide quick responses during early stages of ship design, a simplified mathematical model is devised to simulate the notional all electric ship thermal behavior both in transient and steady state regimes. The problem consists of computing the temperature and relative humidity distributions around or inside all electric ships. These distributions are determined by external environmental conditions, and by the geometrical distribution of the ship's internal components, which in addition, can generate heat. The internal temperature and relative humidity internally should not exceed the components and internal compartments desired operating conditions, and externally should not leave a recognizable ship's signature.

A three-dimensional cell centered finite volume scheme was used to discretize the domain and numerically solve the problem [10]. The innovation in the present model is that a coarse mesh is built with lumped control volumes. The procedure produces results accurate enough for design and optimization purposes. This is possible once that theoretical and empirical heat transfer correlations available in the literature are utilized to simplify the modeling equations, stabilize and speed up the computations. The control volumes consist of bounding boxes that contain either a fluid (e.g., air, water) and/or solid equipment.

Since the main objective is to obtain accurate temperature and relative humidity distributions, whenever forced convection is present, the required flow field in the domain is imposed approximately, based on the knowledge of external environmental conditions (e.g., wind and sea water speed) and internal components (e.g., mass flow rates, fans, turbines). Therefore, the governing equations are only the mass and energy conservation principles applied to each volume element.

The combination of the proposed simplified physical model with the adopted finite volume scheme for the numerical discretization of the differential equations is called a volume element model (VEM). The model takes into account the existence of element internal heat sinks (or sources) and the heat transfer processes across the six element faces, by conduction, convection and radiation (e.g., sun incidence on the domain boundaries).

The model was published previously by the authors [1-3], and was validated experimentally for electronic packages by direct comparison with laboratory measurements [1]. Although the model has simplifying assumptions, the experimental validation demonstrated that the model captures the expected system physical trends, and is accurate enough, so that it could be used for ship design, simulation, control and optimization purposes. Therefore, in this work the model introduced previously by the authors [1-3] has been improved to include fresh and sea water cooled systems throughout the ship.

The main features of the previously presented model [1-3] are summarized for clarity since it has been adapted to the notional all electric ship in the present work. However, the new equations are presented in detail.

Figure 1 summarizes the distribution of the components of the notional all-electric ship baseline medium voltage direct current (MVDC) architecture, their respective zones, and a proposal for the general cooling strategy, including sea water, fresh water and air conditioning cooling systems. The larger loads are shown individually (e.g., gas turbines, pulse load), whereas the smaller loads have been lumped for simplicity in auxiliary sea water (blue), fresh water (green) and air conditioning (violet) cooled loads.
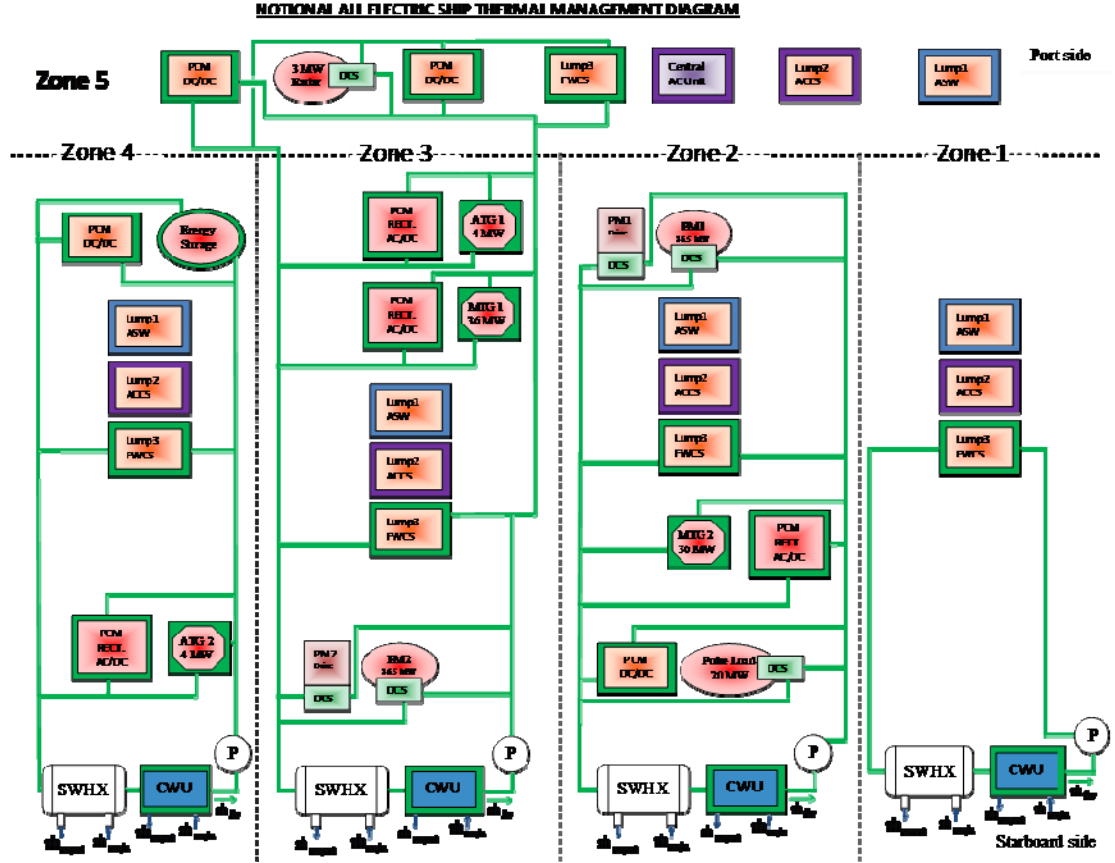
Figure 1. Schematic diagram of notional equipment and cooling circuits, where AC – air conditioning; ACCS – air conditioned cooled system; AC/DC – alternating to direct current; ASW – auxiliary sea water cooled; ATG – auxiliary gas turbine; CWU – chilled water unit; DCS – dedicated cooling system; FWCS – fresh water cooled system; ṁ – mass flow rate; MTG – main gas turbine generator; P – pump; PCM – power conversion module; PM – propulsion motor; RECT – rectifier, and SWHX – sea water heat exchanger.

The notional all electric ship thermal management diagram presented in Fig. 1 was conceived based on the baseline medium voltage direct current (MVDC) architecture proposed by the ESRDC electrical engineering team, which is shown in Fig. 2.

Figure 3 shows a typical cell (or volume element) that may contain either fluid and/or solid material, according to the element type. Each element interacts with the other adjacent elements, according to the energy equation (first law of thermodynamics) applied to the cell, as follows:

$$\frac{dT_i}{dt} = \frac{1}{(\rho\,V\,c)_i}\left(\sum_{j=e,w,t,b,n,s}\dot{Q}_j + \dot{Q}_{gen} + \dot{Q}_{conv}\right)_i \quad (1)$$

where $1 \le i \le N$, with N being the total number of elements in the mesh, T_i are the temperatures of each volume element, ρ is the density of the material inside the volume element (fluid and/or solid), V is the total cell volume, c is

either the specific heat of the solid/liquid or the specific heat at constant volume of the gas inside the volume element (c_v), $\dot{Q}_e$, $\dot{Q}_w$, $\dot{Q}_t$, $\dot{Q}_b$, $\dot{Q}_n$, $\dot{Q}_s$ and $\dot{Q}_{gen}$ are the heat transfer rates across the east, west, top, bottom, north, south faces of each volume element and the heat sink or source inside the element, respectively, and $\dot{Q}_{conv}$ is the net heat transfer rate collected/rejected through convection by one or more fluid streams (fresh or sea water) that flow through the volume element.

The system of ordinary differential equations defined by Eq. (1) formulates the initial value problem to be solved, depicting the temperature field inside the ship at any instant of time, for given initial conditions T_{i0}.

Next, the relative humidity at each air element (relative humidity field) follows from the temperature field, by assuming a known initial relative humidity field.

The relative humidity at any instant of time follows from the temperature field, for a given initial relative

humidity condition, ϕ_{i0}. First, the initial vapor pressure is calculated as follows:

$$p_{v,i} = \phi_{i0} \cdot p_{vs}(T_{i0}) \qquad (2)$$

where $p_{v,i}$ is the cell partial vapor pressure, ϕ_{i0} is the cell initial relative humidity, $p_{vs}(T_{i0})$ is the water saturation pressure at T_{i0}.

It is assumed that the absolute humidity in each volume element remains approximately constant during the whole simulation. Hence, the relative humidity at each element that contains air is computed from

$$\phi_i = \frac{p_{v,i}}{p_{vs}(T_i)} \qquad (3)$$

where ϕ_i is the relative humidity of the cell and $p_{vs}(T_i)$ is the water saturation pressure at temperature T_i. When the element contains solid equipment (or liquids) a zero value is assigned to it, i.e., $\phi_i = 0$.
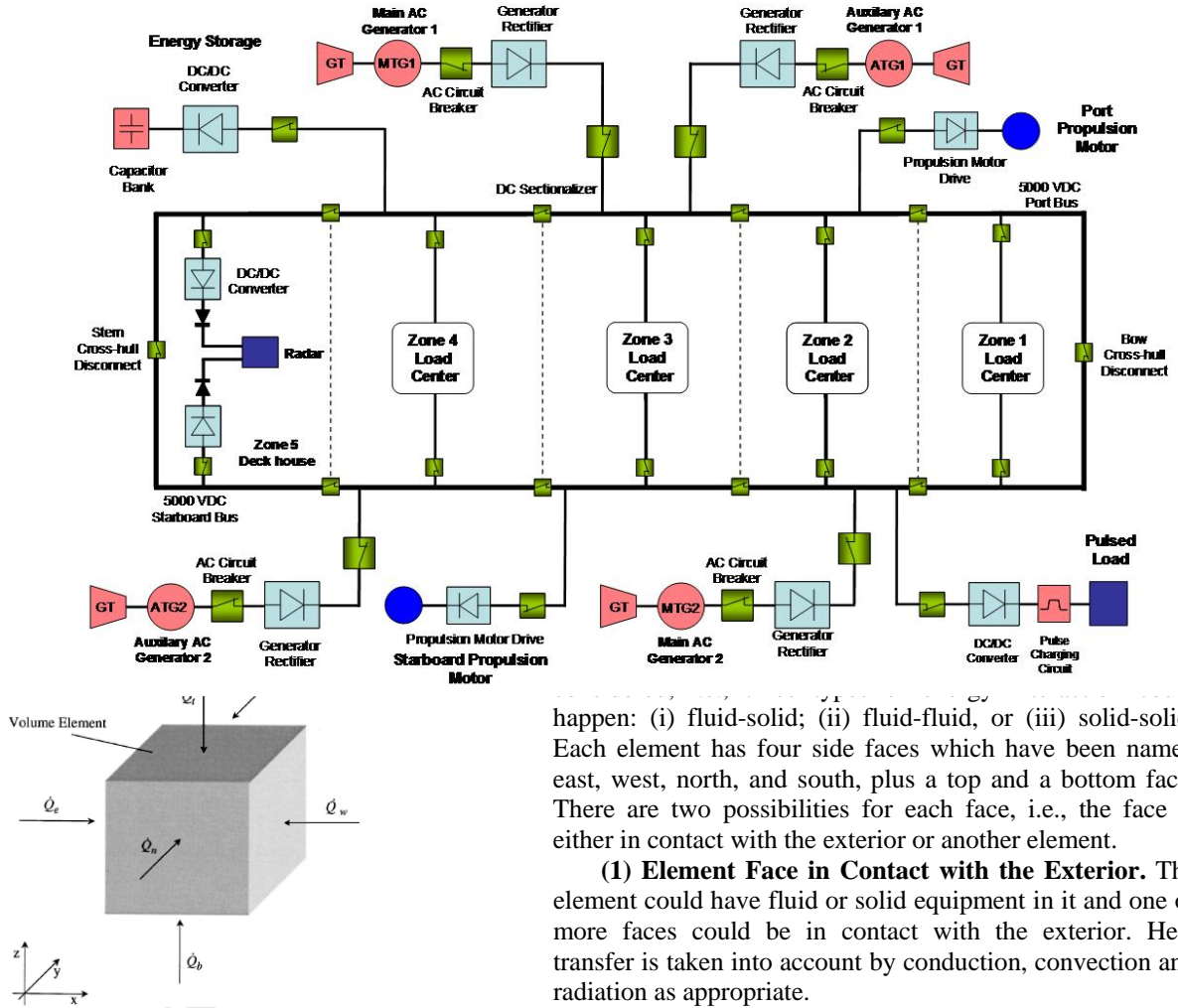

Figure 3. Typical volume element (VE) with heat transfer interactions.

2.1. Heat transfer rates across the element faces

Empirical correlations [11, 12] are utilized to calculate the heat transfer rates across the faces of each volume element (VE). The possible alternatives have been happen: (i) fluid-solid; (ii) fluid-fluid, or (iii) solid-solid. Each element has four side faces which have been named east, west, north, and south, plus a top and a bottom face. There are two possibilities for each face, i.e., the face is either in contact with the exterior or another element.

(1) Element Face in Contact with the Exterior. The element could have fluid or solid equipment in it and one or more faces could be in contact with the exterior. Heat transfer is taken into account by conduction, convection and radiation as appropriate.

The radiation heat transfer rate across the element face is calculated by:

$$\dot{Q}_{rad,i,j} = A_{i,j}\left\{\alpha_j I - \varepsilon_j \sigma\left(T_{i,j}^4 - T_{ext}^4\right)\right\} \ , \quad j = e,w,n,s,t,b \qquad (4)$$

where the first term in the curly brackets represents the portion of the average sun irradiation [13] absorbed by the face, when there is sun incidence; $T_{ext} = T_\infty$ (exterior air temperature) or $T_{ext} = T_{sea}$ (sea water temperature), α and ε

are the element face absorptivity and emissivity, respectively, σ is the Stefan-Boltzman constant, and $A_{i,j}$ is the element face area. It is also assumed that $I = 0$ at the surfaces in contact with sea water.

The conduction and convection heat transfer rate across the face of the element is therefore computed as follows:

$$\dot{Q}_{i,j} = \dot{Q}_{rad,i,j} + U_{i,j} A_{i,j} (T_{ext} - T_i), \quad j = e, w, n, s, t, b \quad (5)$$

where the global heat transfer coefficient, $U_{i,j}$, is given by

$$U_{i,j} = \frac{1}{R_{i,j}} \quad (6)$$

$$R_{i,j} = \frac{l_{i,j}/2}{k_i} + \frac{t_w}{k_w} + \frac{1}{h_{ext}} \quad \text{(solid VE)} \quad (7)$$

or

$$R_{1,i} = \frac{1}{h_{int}} + \frac{t_w}{k_w} + \frac{1}{h_{ext}} \quad \text{(air VE)} \quad (8)$$

where $l_{i,j}$ is either the cell length or width, k_i is the cell thermal conductivity, t_w and k_w are the wall thickness and thermal conductivity, respectively, h_{int} and h_{ext} are the interior and exterior convection heat transfer coefficients.

The heat transfer coefficient, h, is calculated for
a) natural convection [11, 12]

$$h = \frac{k_f}{H} \left\{ 0.825 + \frac{0.387 \, Ra_H^{1/6}}{\left[1 + (0.492/Pr)^{9/16} \right]^{8/27}} \right\}^2 \quad (9)$$

where k_f is the fluid thermal conductivity, Pr is the Prandtl number of the fluid and $Ra_H = \frac{g\beta}{\alpha_T \nu} H^3 |T_{neigh,i} - T_i|$, g is the gravity, β is the fluid coefficient of thermal volumetric expansion, α_T is the fluid thermal diffusivity, ν is the fluid kinematic viscosity, $T_{neigh,i}$ is the temperature in the neighbor VE or the exterior temperature, and H is the total solid swept height under analysis.

Equation (9) is valid for the entire Rayleigh number range—laminar, transition and turbulent—with the fluid properties evaluated at the film temperature, i.e., $T_{film} = (T_{neigh,i} + T_i)/2$, for all Prandtl numbers [14].

b) forced convection [11, 12]

$$h = \frac{k_f}{L} \left(0.064 \, Pr^{1/3} \, Re_L^{1/2} \right), \text{ for } Re_L < 5 \times 10^5 \quad (10)$$

or

$$h = \frac{k_f}{L} \left\{ 0.037 \, Pr^{1/3} \left(Re_L^{4/5} - 23550 \right) \right\}, \text{ for } Re_L > 5 \times 10^5 \quad (11)$$

where $Re_L = \frac{v_f L}{\nu}$, v_f is the fluid velocity, and L is the total solid swept length under analysis.

(2) Side Face in Contact with Another Element. The element could have fluid or solid equipment inside. In both cases only conduction takes place between adjacent elements, if the two elements have fluid (i.e., no relative motion between fluid layers) or solid equipment inside. The other possibility is a fluid/solid equipment interaction between the two elements, then heat transfer across the element face is ruled by convection.

For the fluid/fluid contact, since it is assumed that the fluid is not moving across the side faces, the heat transfer rate is given by

$$\dot{Q}_{1,i} = - U_{1,i} A_{1,i} (T_i - T_a), \quad l = e, w, n, s \quad (12)$$

where a is the number of the adjacent element, and

$$U_{1,i} = \frac{k_f}{(l_{m,i} + l_{m,a})/2} \quad (13)$$

where $l_{m,i}$ and $l_{m,a}$ are either the cell length or width, according to the index $m = x$ or y, if the "i-th" or "a-th" cell side face is east/west or north/south, respectively.

For the solid/solid contact, the heat transfer rate is also obtained from Eq. (12), in which this time

$$U_{1,i} = \frac{1}{\frac{l_{m,i}/2}{k_i} + \frac{l_{m,a}/2}{k_a}} \quad (14)$$

When the contact is of the type fluid/solid equipment, convection takes place. Equation (12) is utilized, and the appropriate heat transfer coefficient, h_l, is computed as in Eqs. (9) – (11), and

$$U_{1,i} = \frac{1}{\frac{1}{h_1} + \frac{l_{m,c}/2}{k_c}} \quad (15)$$

where the index c is the number of the solid element.

(3) Top/Bottom Face in Contact with Another Element. Since any element could have fluid or solid equipment inside, three types of interaction have to be taken into account, i.e., (i) fluid/fluid, (ii) fluid/solid, and (iii) solid/solid.

(i) fluid/fluid

Both elements have fluid inside, and the heat flux is given by

$$\dot{Q}_{1,i} = \dot{m}_{1,i} \, c_{p,f} (T_a - T_i), \quad l = t, b \quad (16)$$

where $\dot{m}_{1,i} = \rho_f \, v_i \frac{A_{1,i}}{2}$.

For natural convection, the estimated fluid velocity crossing the element face is $v_i = \alpha_T \left(\frac{g\beta}{\alpha_T \nu} |T_a - T_i| H \right)^{1/2}$, which is a natural convection representative scale [11, 12]. It is also assumed that half of the element top/bottom face is crossed by the fluid in the upward direction, and the other half in the opposite direction.

In case of forced convection, the estimated fluid velocity crossing the element face, v_i, is a known parameter from the air conditioning system design.

(ii) fluid/solid

The heat transfer rate across the top/bottom element face follows from Eq. (12), with $l = t, b$. $U_{l,i}$ is computed with Eq. (15), and $l_{m,c}$ is replaced by $l_{z,c}$.

(iii) solid/solid

When both elements are solid pieces of equipment, the heat transfer rate also follows from Eq. (12), with $l = t, b$. $U_{l,i}$ is given by Eq. (15), and the lengths $l_{m,i}$ and $l_{m,a}$ are replaced by $l_{z,i}$ and $l_{z,a}$, respectively.

2.2. Heat transfer rates collected/rejected by fresh or sea water systems

In order to account for the different ship components and their cooling strategies, 6 (six) volume element types are defined based on its contents: 0) only air; 1) pure solid; 2) sea water heat exchanger (SWHX); 3) chilled water units (CWU); 4) fresh water cooled systems, and 5) sea water cooled systems.

For element types 0 and 1, in Eq. (1), $\dot{Q}_{conv} = 0$, since there are no fresh or sea water streams flowing across them. However, for element types 2 to 5, $\dot{Q}_{conv}$ is not zero and is a result of the adopted ship cooling strategy.

In the notional ship cooling system modeled in Figure 1, each zone is cooled separately, with a combined air conditioning, sea and fresh water cooling strategy. The system may contain cross-connects between zones to increase redundancy; these are not modeled in this work as this system is not designed to normally operate in a cross-connected manner. According to Fig. 1, each ship zone has a sea water heat exchanger (SWHX), a chilled water unit (CWU) and a pump set, which are mounted in series, so that the fresh water flows in a closed loop collecting heat from the heat generating zone systems. In this way, the hot fresh water stream rejects heat to the cold sea water stream in the sea water heat exchanger (SWHX). Next, the fresh water is further cooled by a chilled water unit (CWU) thereafter returning to the zone interior where it will serve as heat sink to the fresh water cooled systems. Although this would not be the typical shipboard system layout, this example allows us to demonstrate modeling two methods of heat removal from chilled water. As shown in Fig. 1, other cooling strategies are also used, such as systems cooled by the air conditioning system (Lump 1) and directly by auxiliary sea water (Lump 2). The expected result of this combined cooling strategy is that the zones and the entire ship temperature and relative humidity fields remain within acceptable and pre-established design limits.

The calculations start with the determination of the fresh water temperature at the SWHX inlet in each ship zone. For that a mixer section is devised before the SWHX inlet, in which the inputs are the mass flow rates that come from the output of each fresh water cooled component in the zone, and the output is the zone total fresh water mass flow rate. Therefore, a balance of energy in such mixer allows for the calculation of the zone fresh water mixer outlet temperature, which is the SWHX inlet temperature, as follows:

$$T_{fw,in} = \frac{\sum_{j=1}^{n_{eq}} \dot{m}_{fw,j} T_j}{\dot{m}_{fw}} \qquad (17)$$

where $\dot{m}_{fw,j}$ is the fresh water mass flow rate coming out of component j; T_j the temperature of component j (assumed equal to the fresh water coming out of it), and $\dot{m}_{fw}$ the total fresh water mass flow rate in the zone.

The heat transfer rates collected/rejected by fresh or sea water, $\dot{Q}_{conv}$, are then calculated for each element type as follows:

(i) Element type 2 (SWHX):

The effectiveness-NTU method [11] is utilized to estimate the SWHX effectiveness, assuming a counterflow heat exchanger through:

$$\varepsilon_{hx} = \frac{1 - \exp\{-NTU(1 - C_{min}/C_{max})\}}{1 - (1 - C_{min}/C_{max})\exp\{-NTU(1 - C_{min}/C_{max})\}} \quad (18)$$

where $NTU = (UA)_{SWHX}/C_{min}$; U and A are the SWHX global heat transfer coefficient and heat transfer area, respectively; $C_{min} = (\dot{m}c)_i$ is the smallest heat capacity between the two streams (i = fresh or sea water) and C_{max} the other one.

From the definition of effectiveness [11] and Equation (18), the SWHX sea water outlet temperature is evaluated as

$$T_{sw,out} = \frac{\varepsilon_{hx} \dot{m}_{fw} c_{fw}(T_{fw,in} - T_{sw,in})}{\dot{m}_{sw} c_{sw}} + T_{sw,in} \qquad (19)$$

where $\dot{m}$ and c are the mass flow rate and specific heat, respectively, T the temperature, subscripts fw, sw, in and out, refer to fresh water, sea water, inlet and outlet, respectively.

Therefore, the net heat transfer rate through the water streams crossing element type 2 is calculated as follows:

$$\dot{Q}_{conv} = \dot{m}_{fw} c_{fw}(T_{fw,in} - T_i) + \dot{m}_{sw} c_{sw}(T_{sw,in} - T_{sw,out}) \ (20)$$

where subscript "i" refers to the element type 2 under analysis, so that T_i is the element temperature which is assumed equal to the fresh water outlet temperature as well, according to the thermodynamic assumption of uniform properties in a control volume.

(ii) Element type 3 (CWU):

The net heat transfer rate through the fresh water stream crossing element type 3 is calculated as follows

$$\dot{Q}_{conv} = \dot{m}_{fw} c_{fw}(T_{SWHX,out} - T_i) \qquad (21)$$

where subscript "i" refers to the element type 3 under analysis, and $T_{SWHX,out}$ is the SWHX outlet temperature.

In element type 3, $\dot{Q}_{gen} < 0$, which is a design parameter corresponding to the nominal refrigeration rate of the selected chilled water unit. In this unit, it is assumed that heat is rejected to a sea water stream that extracts heat from the condenser.

(iii) Element type 4 (fresh water cooled components):

The net heat transfer rate through the fresh water stream crossing any element type 4 in the zone is calculated as follows

$$\dot{Q}_{conv} = \dot{m}_{fw} c_{fw} \left(T_{CWU,out} - T_i \right) \tag{22}$$

where subscript "i" refers to the element type 4 under analysis, and $T_{CWU,out}$ is the CWU outlet temperature.

As shown in Fig. 1, some components have dedicated cooling systems, which could be a refrigeration system or a deionized water heat exchanger. In the case of a dedicated refrigeration system, heat is extracted from the load through the evaporator, but the heat transfer rate that is rejected by the condenser inside the element is given by:

$$\dot{Q}_{gen} = \frac{1+\eta}{\eta} \dot{Q}_{evap,DCS} \tag{23}$$

where $\dot{Q}_{evap,DCS}$ is a design parameter corresponding to the nominal refrigeration rate of the refrigeration unit that was selected to cool the load locally which is meant to match the component heat generation rate, and η is the nominal unit thermal efficiency (or COP – coefficient of performance).

In the case of a deionized water heat exchanger, $\dot{Q}_{gen}$ is assumed to be the component heat generation rate.

(iv) Element type 5 (auxiliary sea water cooled systems – ASW)

The net heat transfer rate through the auxiliary water stream crossing any element type 5 in the zone is calculated as follows

$$\dot{Q}_{conv} = \dot{m}_{sw} c_{sw} \left(T_{sw,in} - T_i \right) \tag{24}$$

where subscript "i" refers to the element type 5 under analysis.

Equation (1) defines a system of N ordinary differential equations with time as the independent variable, along with the initial conditions, for the unknowns T_i , i.e., the temperatures at the center of each volume element. Once the temperatures at the center of each volume element are known, the corresponding relative humidity follows immediately from Eqs. (2) and (3).

3. NUMERICAL METHOD

The unsteady system of equations is integrated in time, from given initial conditions, explicitly using a 4th order Runge-Kutta method [15]. If the transient solution is of no interest, the system is solved directly for the steady-state solution. The time derivative terms in the ODE's system defined by Eq. (1) are dropped and a system of N nonlinear algebraic equations is obtained. In this case the unknowns are the steady-state temperatures at the center of each elemental volume. The resulting nonlinear system of algebraic equations is solved using a Newton-Raphson method. The system of equations is linearized with respect to the cell center temperatures, after which the volume elements relative humidities are computed based on Eqs. (2) and (3). In the cases studied in this paper, the iterative process required 5 to 10 min to achieve convergence, i.e., the Euclidean norm of the residual of the system was less than 10^{-3}. Hence a low computational time to obtain the steady-state solution was required in all cases. The computer used to perform the simulations was a laptop with a Pentium (R) Dual-Core CPU T4300 @ 2.10 GHz, 3 GB RAM, 64-bit operating system.

All simulations were performed in a LINUX operating system. A C++ code was written to produce the tridimensional mesh to represent the ship as a computational domain. Numerical results were produced with a Fortran code based on the mathematical model described in Section 2. The input data for the computational simulation of the systems response were selected according to the geometry, components, operating and environmental conditions of the case studies simulated in this paper. The convergence of the numerical results was verified by successive mesh refinements [16] and monitoring the variation of the Euclidean norm of the temperatures numerical solution in the entire domain. The results of a less refined mesh (mesh 1) are compared to the results of a more refined mesh (mesh 2), and the refinements stop when the mesh refinement relative error, ε_{mesh}, criterion is satisfied, then mesh 1 is selected as the converged mesh, as follows:

$$\varepsilon_{mesh} = \frac{\left| \|T\|_{mesh1} - \|T\|_{mesh2} \right|}{\|T\|_{mesh1}} \le 0.01 \tag{25}$$

Both the mesh and the numerical results were processed for graphical visualization in different planes and surfaces. For that, a free graphic software produced by the Lawrence Livermore National Laboratory was utilized [4].

4. RESULTS AND DISCUSSION

The ship is divided into small compartments (volume elements) and equipments are placed in one or more grid elements according to their actual dimensions. The procedure was designed to start with the x, y and z coordinates of a particular equipment, listed in the notional data [17] which are then compared with the midpoint coordinates of all grid elements in order to determine to which grid elements the equipment should be allocated.

In the present work, in order to assess conceptually the possibility of obtaining the ship's internal temperature distribution with the proposed model and computational application, the notional all electric ship baseline medium voltage direct current (MVDC) architecture presented in

Fig. 2 was utilized. So, instead of using the loads from the database [17], all of them were lumped in their respective zones with an estimated total value. Besides the loads of the database, all ship loads shown in Fig. 2 were accounted for in the simulations.

The ship discretization follows the notional data standards showed in Fig. 4. The ship geometry has 11 deck divisions (4 below and 7 above watertight), 200 divisions in the bow to stern direction and 7 divisions in the port to starboard direction.
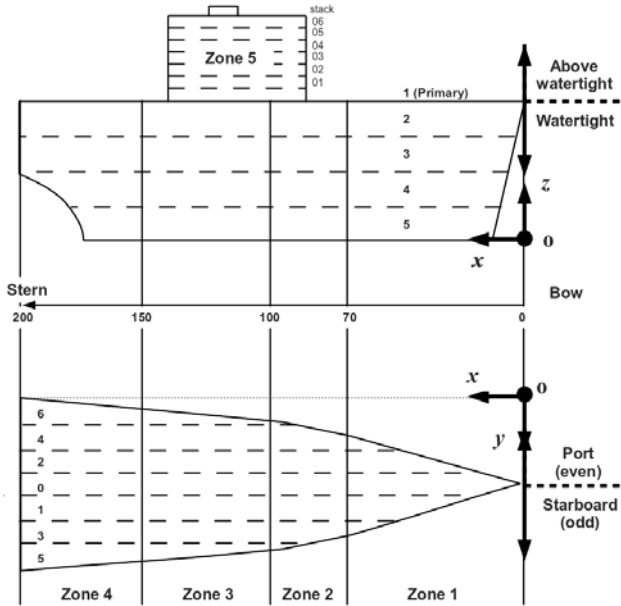

Figure 4. Ship zones distribution.

The resulting 3D geometry is shown Fig. 5. The converged grid according to the criterion of Eq. (25) had a total of 9410 elements. Grid generation was constructed with the notional ship physical dimensions [17]. The notional all-electric ship geometric dimensions are shown in Table 1.

The external conditions considered in the two simulations performed in this work are: frontal wind speed – 10 m/s; frontal speed – 10 m/s, air temperature of 260 and 305 K, and sea water temperature of 280 and 288 K, for 10 and 90 ^{o}F days, respectively. The mesh was non-uniform, i.e., the cells had variable sizes to allow for the representation of the ship in the domain, and to place the heat generation sources appropriately in each ship zone. The notional all electric ship equipment list per zone, and respective heat generation rate are shown in Table 2.
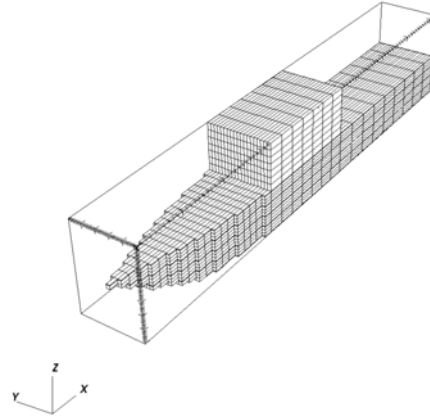

Figure 5. Notional ship converged mesh.

Table 1. Notional all electric ship dimensions.

direction	length (m)	divisions
bow to stern (length)	184	200
port to starboard (beam)	24	7
baseline to watertight deck (depth)	16	4
watertight deck to top of superstructure	18	7

Regarding the thermal design, sea water heat exchangers (SWHX) with known global heat transfer coefficients, U [W m^{-2} K^{-1}], and areas, A [m^2], were allocated to zones 1, 2, 3-5, and 4, such that (U, A) = (100, 100); (100, 500); (100, 1000), and (100, 100), respectively. Also chilled water units (CWU) were allocated to zones 1, 2, 3-5, and 4, with known refrigeration capacity rates of 100, 500, 500, and 100 kW, respectively. Finally, equal fresh and sea water total mass flow rates of 8, 60, 60, and 10 kg s^{-1} were selected to zones 1, 2, 3-5, and 4, respectively.

Figure 6 shows the spatial distribution of all pieces of equipment listed in Table 2 inside the ship. Arbitrary locations and dimensions were selected to conduct the simulations presented in this work. However, the equipment locations and dimensions can be easily changed in the input data according to any mechanical notional ship design.

In both scenarios analyzed in this work, it was assumed that the ship's hull was 10 m underwater, and the assumed known initial relative humidity was $\phi_{i0} = 0.08$ (80 %). Only steady state simulations were performed in this study.

| Electrical Equipment	Power (kW)	Efficiency	Heat Generation Rate (kW)
Table 2. Notional all electric ship equipment list.			
			Zone 5
RADAR PCM DC/D	3866	0.97	115.98
RADAR	3750	0.85	562.5
Lump1 (ASW)			30
Lump2 (ACCS)			10
Lump3 (FWCS)			30
TOTAL			**748.48**
			Zone 4
ATG2	4000	0.96	160
PCM AC/DC	3840	0.96	153.6
ES PCM DC/DC	4000	0.97	120
Lump1 (ASW)			100
Lump2 (ACCS)			200
Lump3 (FWCS)	2965	0.85	444.75
TOTAL			**1178.35**
			Zone 3
MTG1	36000	0.98	720
PCM AC/DC	35280	0.98	705.6
ATG1	4000	0.96	160
PCM AC/DC	3840	0.96	153.6
PORT Motor Drive	37200	0.98	744
PORT Motor	36500	0.98	730
Lump1 (ASW)			200
Lump2 (ACCS)			200
Lump3 (FWCS)	3890	0.85	583.5
TOTAL			**4196.7**
			Zone 2
MTG2	36000	0.98	720
PCM AC/DC	35280	0.98	705.6
STBD Motor Drive	37200	0.98	744
STBD Motor	36500	0.98	730
Pulsed Load (FEL)	25000	0.12	36.67
Lump1 (ASW)			100
Lump2 (ACCS)			200
Lump3 (FWCS)	3241	0.85	486.15
TOTAL			**3722.4**
			Zone 1
Lump1 (ASW)			36.27
Lump2 (ACCS)			50
Lump3 (FWCS)	2790	0.85	418.5
TOTAL			**504.77**
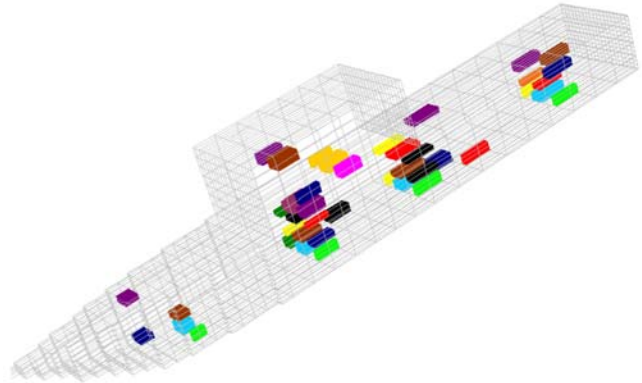
Figure 6. Components distribution inside the ship.

The resulting external temperature field for the first simulation in a 10 $^{\circ}$F day is shown in Figure 7. The maximum observed temperature within the ship was 373.4 K, as it is shown in the legend of Fig. 7, which demonstrates the effectiveness of the fresh and sea water cooling strategies to extract the large heat generation rates shown in Table 2 out of the ship, and keeping the cooling water temperature below boiling point throughout the ship. The constraints in this model were set to maintain chilled water below boiling; these constraints can be changed as required for actual system specifications.
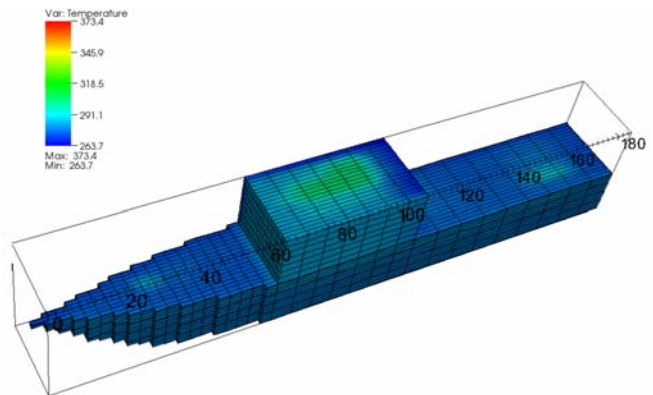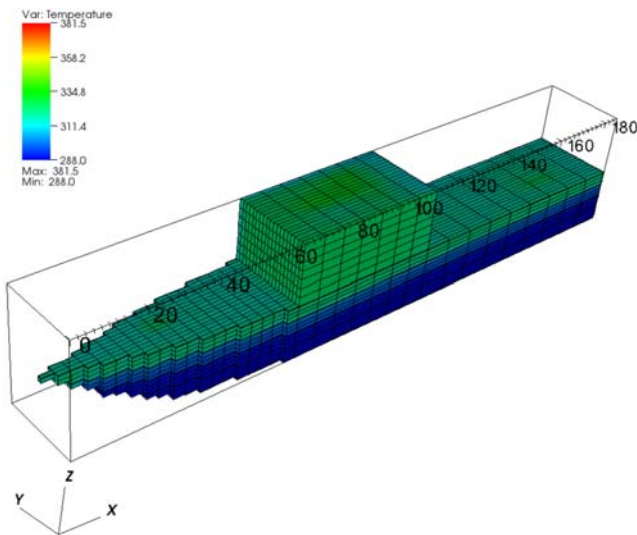

Figure 7. Ship external temperature field (10 $^{\circ}$F day).

The results are further analyzed internally in the ship midplane in Fig. 8. As expected the highest temperatures occur in zones 2 and 3 where heat generation is higher.
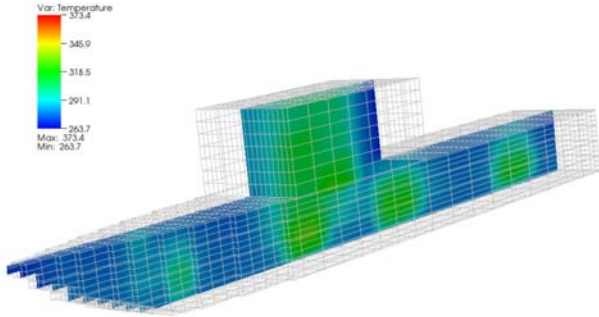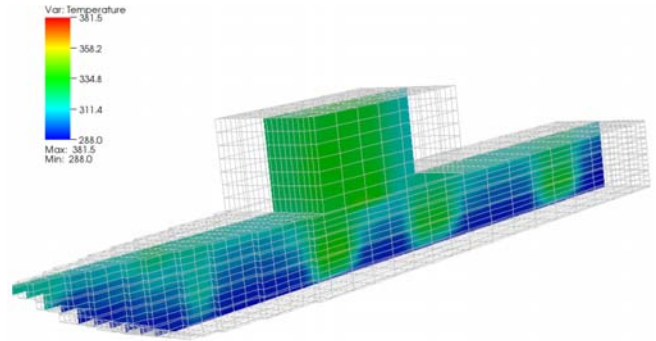
Figure 8. Ship midplane temperature field (10 ^{o}F day).

The resulting external temperature field for the second simulation in a 90 ^{o}F day is shown in Figure 9. The maximum temperature within the ship was 381.5 K (above water boiling point), and was registered in a volume element that did not contain water, as it is shown in the legend of Fig. 9, which again demonstrates the effectiveness of the water cooling strategies to extract heat out of the ship, even in a hotter day than the previous simulation. In this simulation, it is possible to notice the water line on the hull through the surface temperature distribution.


Figure 9. Ship external temperature field (90 ^{o}F day).

Next, the results are analyzed internally in the ship midplane in Fig. 10a. Again, the highest temperatures occur in zones 2 and 3 where heat generation is higher. Figure 10b illustrates the resulting humidity field in the ship's midplane. It is interesting to note that as temperature increases, the relative humidity decreases in air volume elements, as expected thermodynamically. Also, in solid volume elements, the model sets $\phi_i = 0$, therefore it is possible to identify where solid equipments are located based on the resulting relative humidity distribution.

(a)
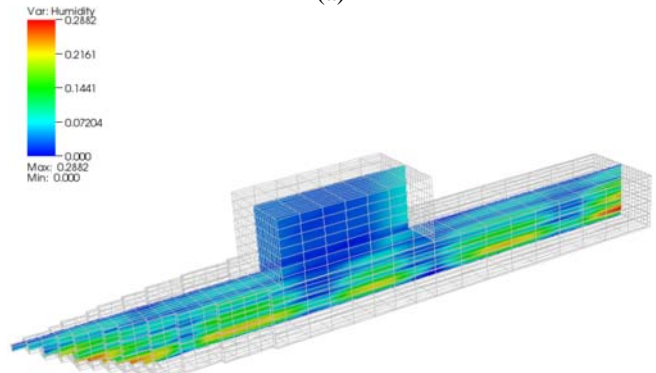
Figure 10. Ship midplane temperature (a) and relative humidity (b) field (90 ^{o}F day).

Finally, one of the main objectives of this work was to develop a computational tool that required low computational time to provide solutions for each tested configuration in order to allow for an effective design and optimization procedure. The largest computational time required for obtaining the results for the cases presented in this work was of 560 s, i.e., less than 10 min, using as initial value, a temperature field in equilibrium with the external environment, which is the expected worst scenario. Whenever solutions are available from previous simulations, the use of restart files dramatically reduces the required computational time for convergence to the new case solution. Based on these observations, it is reasonable to state that such objective has also been accomplished.

5. CONCLUSIONS

In this paper, a general transient computational model for the thermal management of physical systems with heat sinks and sources, fresh and sea water, as well as air conditioning cooling strategies has been developed. The model was tested with steady state simulations of a notional all electric ship. The obtained results illustrate how the VEM could be used to calculate the temperature and relative humidity fields anywhere in the domain, for any number of volume elements adopted in the simulations. The model

allows for the use of a relatively coarse mesh to discretize the domain and still obtain converged numerical results, with low computational time, in spite of the diverse nature of the components inside the domain. Therefore it is expected that, after experimental validation and model adjustment to ensure the accuracy of results, the developed application could be used as an efficient tool for ship thermal design, control and optimization.

6. ACKNOWLEDGEMENT

7. REFERENCES

[1] Vargas, J. V. C., Stanescu, G., Florea, R., and Campos, M. C., 2001, "A Numerical Model to Predict the Thermal and Psychrometric Response of Electronic Packages," ASME Journal of Electronic Packaging, 123, no. 3, 200-210.

[2] J. C. Ordonez, J. V. C. Vargas, R. Hovsapian, 2008, "Modeling and Simulation of the Thermal and Psychrometric Transient Response of All-Electric Ships, Internal Compartments and Cabinets," Simulation, 84, no. 8-9, 427-439.

[3] Dias, F. G., Souza, J. A., Ordonez, J. C., Vargas, J. V. C., Hovsapian, R. and Amy Jr, J. V., 2009, "Notional All-Electric Ship Thermal Simulation and Visualization." In: Proceedings of the 2009 IEEE Electric Ship Technologies Symposium, Baltimore, Maryland. 2009 ESTS Proceedings. New York: IEEE.

[4] VisIt 1.11.1 Manual, 2008, Lawrence Livermore National Laboratory, Livermore, CA, USA.

[5] Souza, J. A., O'Lary, F. M., Hovsapian, R., Ordonez, J. C. Vargas, J. V. C. and Chalfant, J., 2010, "Visualization Tool for Notional All-Electric Ships Data Bases." In: Proceedings of the 2010 Grand Challenges in Modeling and Simulation, Ottawa, Canada. 2010 GCMS Proceedings, July 11 – 14.

[6] Wagner, B., 2007, "All-Electric Ship Could Begin to Take Shape By 2012," NDIA's Business and Technologies Magazine, November.

[7] Smith, A. N., Ellis, R. L., Bernardes, J. S., Zielinski, A. E., 2005, "Thermal Management and Resistive Rail Heating of a Large-Scale Naval Electromagnetic Launcher," IEEE Transactions on Magnetics, 41, no. 1, 235-240.

[8] Kanerva, S. and Hansen, J. F. , 2009, "State of the Art in Electric Propulsion - Viewpoint on Redundancy." In: IEEE Electric Ship Technologies Symposium, 499-504, Baltimore, Maryland, USA.

[9] Soman, R. R., Davidson, E. M., McArthur, S. D. J., "Using Functional Failure Mode and Effects Analysis to Design the Monitoring and Diagnostics Architecture for the Zonal MVDC Shipboard Power System." In: IEEE Electric Ship Technologies Symposium, 123-128, Baltimore, Maryland, USA.

[10] Fletcher, C. A. J. 1991. Computational Techniques for Fluid Dynamics, vol. 1, Springer-Verlag, Berlin.

[11] Bejan, A. 1993. Heat Transfer, Wiley, New York.

[12] Bejan, A. 1995. Convection Heat Transfer, 2nd Ed., Wiley, New York.

[13] Duffie, J. A. and Beckman, A. A. 1974. Solar Energy Thermal Processes, Wiley, New York, 34–37.

[14] Churchill, S. W. and Chu, H. H. S., 1975, "Correlating Equations for Laminar and Turbulent Free Convection from a Vertical Plate," Int. J. Heat Mass Transfer, 18, 1323–1329.

[15] Kincaid, D. and Cheney, W. 1991. Numerical Analysis, Wadsworth, Belmont, CA.

[16] Editorial, 1994, "Journal of Heat Transfer Editorial Policy Statement on Numerical Accuracy," ASME J. Heat Transfer, 116, 797–798.

[17] Amy, J., 2008, "Load Analysis 2007 for ESRDC3 REV2.xls", Electric Ship Research and Development Consortium.